Mechanical Properties and Morphology of PP/ABS Blends Compatibilized with PP-*g*-2-HEMA

Alpesh C. Patel, Ragesh B. Brahmbhatt, Surekha Devi

Department of Chemistry, Faculty of Science, M. S. University of Baroda, Vadodara 390 002, India

ABSTRACT: Polypropylene (PP) and acrylonitrile–butadiene–styrene blends of different composition were prepared using a single-screw extruder. The binary blend of PP/ABS was observed to be incompatible and shows poor mechanical properties. PP-*g*-2-hydroxyethyl methacrylate (2-HEMA) was used as a compatibilizer for the PP/ABS blends. The ternary compatibilized blends of PP/ABS/PP-*g*-2-HEMA showed improvement in the mechanical properties. Electron micrographs of these blends showed a homogeneous and finer distribution of the dispersed phase. The mechanical performance increased particularly in the PP-rich blend. The 2.5-phr (part per hundred of resin) compatibilizer was observed to bring improvement to the properties. The suitability of various existing theoretical models for the predication of the tensile moduli of these blends was examined. © 2003 Wiley Periodicals, Inc. J Appl Polym Sci 88: 72–78, 2003

Key words: poly(propylene) (PP); blends; compatbilization; morphology

INTRODUCTION

The field of materials has been a major thrust area in science and technology for the last few decades. In polymeric materials, polymer blends and alloys occupy a special place. The mechanical and morphological properties of the blends depend mainly upon the extent of the homogeneity and adhesion at the interface and the size of the dispersed phase.[1–5]

The homogeneity of polymer blends depends on the mutual solubility of the polymeric components. However, most of the polymer pairs tend to be immiscible due to the difference in viscoelastic properties, surface tension, and intermolecular interactions. To reduce the surface tension and to increase molecular interactions, a third component known as a compatibilizer is used. Block, graft, and star-shaped copolymers are extensively used as compatibilizers for various blends.[1–4,6]

Polyolefin-based binary and ternary blends of polypropylene (PP) and nylon-6,[7] PP and polycarbonate,[8] and PP and poly(ethylene terephthalate)[9] are well studied. However, very little work has been done in the area of PP/acrylonitrile–butadiene–styrene (ABS) blends and has concentrated mainly on improving the compatibility of PP/ABS by using polyethylene (PE) or various SEBS-type block copolymers.[10–18] Work on PP and ABS blends was first published by Markin and William in 1980.[10] They studied the mechanical and rheological properties and melt viscosities of PP and ABS blends in various ratios. Gupta et. al.[11,12] used PE as a third component in PP/ABS blends, with the expectation of better miscibility of the butadiene part of ABS with PE. But not much improvement in the mechanical properties of these blends was observed even upon addition of PE as a third component. Frounchi and Burford[13] studied PP/ABS blends using ethylene–vinyl acetate as a compatibilizer. They observed improvement in the mechanical properties, particularly in the impact strength and tensile strength of PP-rich blends. However, no improvement in the mechanical properties of ABS-rich blends was reported.

An improvement in the impact strength to 5–10 times that of virgin PP was reported for the PP/ABS blends containing compatibilizers such as PP-*g*-maleic anhydride,[19] the ethylene–propylene block copolymer,[20] the butadiene–styrene block copolymer,[21] and the ethylene–vinyl acetate copolymer.[22]

In our earlier report on PP/ABS blends, we examined the role of PP-*g*-acrylic acid as a compatibilizer for the blends.[23] The finer and homogeneous distribution of ABS as a dispersed phase in the PP matrix and improvement in the mechanical performance was observed when the blends were compatibilized with PP-*g*-acrylic acid.

The miscibility of acrylate polymers such as PMMA and MMA–GMA blends with ABS was reported by Fowler et al.[24] and Lee et al.[25] The miscibility of poly-acrylate/ABS was also reported by other workers.[26,27] However, use of 2-hydroxyethyl methacrylate (2-

HEMA) for the compatibilization has not been explored yet. Hence, in this work, we examined PP/ABS blend compatibilization through PP-*g*-HEMA as a compatibilizer.

EXPERIMENTAL

Materials

Isotactic PP of M0030 Koyelene grade with a density of 0.93 g/cm^3 and a melt-flow index 10 g/10 min was supplied by Indian Petrochemicals Corp. Ltd. (Vadodara, India). ABS of 100N grade with a 1.05 g/cm^3 density and a melt-flow index of 10 g/10 min was a gift sample from Bayer–ABS Ltd. (Vadodara, India). 2-HEMA from Fluka (Switzerland) was used after vacuum distillation. Benzoyl peroxide (BPO) and AR-grade toluene and methanol from Qualigens (Mumbai, India) were used as received.

Grafting of 2-HEMA on *in situ* chlorinated PP through solution polymerization was carried out as described earlier.[28] The graft copolymer PP-*g*-2-HEMA was synthesised in bulk at optimized reaction conditions: a 110°C reaction temperature, an 8.2-mM benzoyl peroxide concentration, 1 w/w PP/2-HEMA, and toluene as the reaction medium.

Blend preparation

Prior to extrusion, PP, PP-*g*-2-HEMA, and ABS were dried in a hot air oven at 70°C for 12 h. The blends were prepared by a melt-extrusion technique using a Brabender single-screw extruder with an *L/D* ratio of 20. All the blends were prepared by a two-step mixing technique. In the first step, PP and PP-*g*-2-HEMA (1:1 w/w ratio) were premixed in the extruder, keeping the temperatures of four zones at 190–200–210–220°C and the screw speed at 50 rpm. In the second step, the resultant mixture was pelletized and a calculated amount was mixed with ABS and PP in the extruder operated at a screw speed 50 rpm and the zone temperatures of 200–220–230–225°C for PP-rich blends

and 220–230–250–240°C for ABS-rich blends. The various blend compositions prepared are given in Table I. The extrudates were cut into pellets. The blend pellets were injection-molded using an ARBURG allrounder 220–90–350 injection-molding machine to obtain the test specimen for the measurements of the mechanical properties.

Characterization

Mechanical properties

The measurement of the tensile properties of the dumbbell-shaped samples was carried out using an Instron 4204 testing machine following the ASTM D638 procedure. A crosshead speed of 0.5 cm/min was used in all the measurements. The notched impact strength was measured following the ASTM D256 procedure using a Ceast impact testing machine. At least five specimens with a 0.025-cm notch radius were tested for each sample at room temperature and the average was considered for further studies.
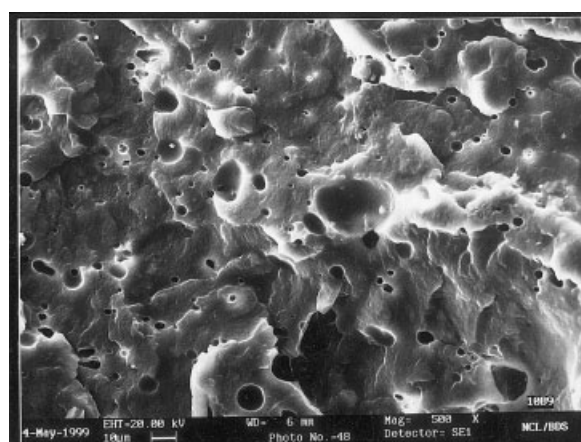
(a)

(b)

Figure 1 Scanning electron micrographs of impact fractured surfaces of the blends: (a) 90/10(%) PP/ABS; (b) 85/15(%) PP/ABS.

TABLE I
Composition of Blends

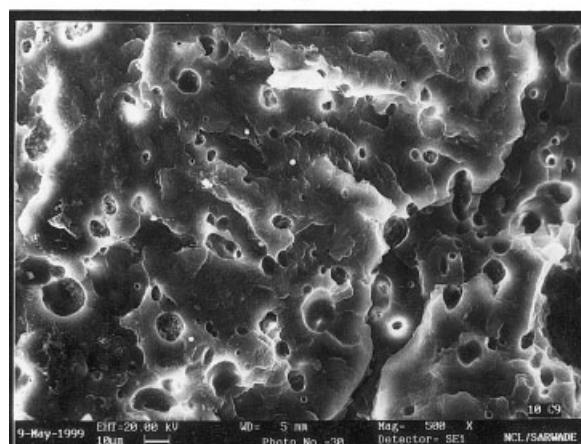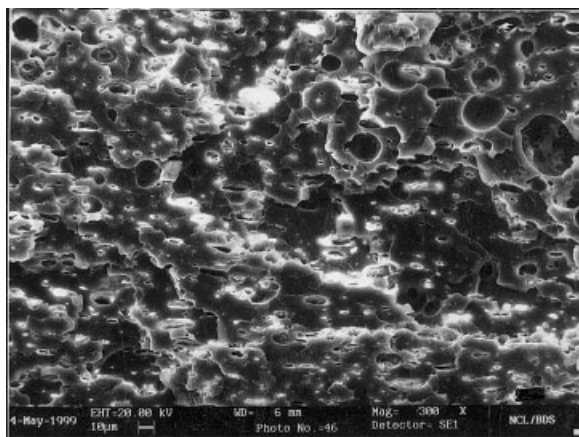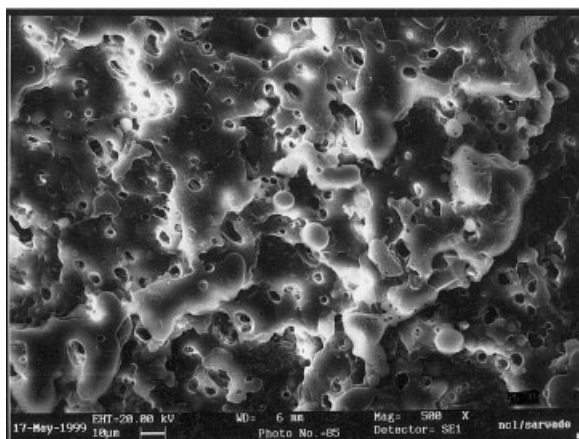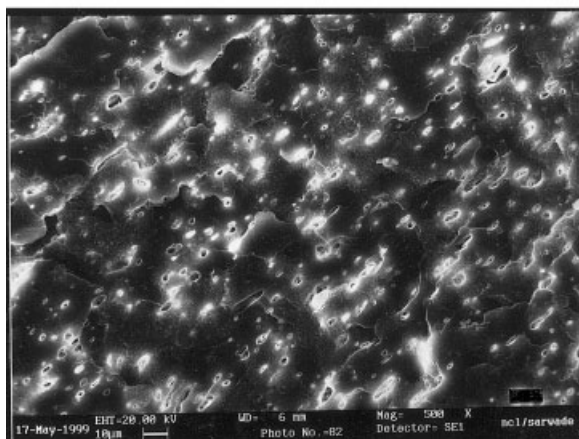| PP/ABS (%)	PP/ABS/PP-*g*-2-HEMA (%)	PP/ABS/PP-*g*-2-HEMA (%)	PP/ABS/PP-*g*-2-HEMA (%)
100/0	—	—	—
90/10	90/10/2.5[a]	90/10/5[a]	90/10/7.5[a]
85/15	85/15/2.5[a]	85/15/5[a]	85/15/7.5[a]
75/25	75/25/2.5[a]	75/25/5[a]	75/25/7.5[a]
25/75	25/75/2.5[a]	25/75/5[a]	25/75/7.5[a]
15/85	15/85/2.5[a]	15/85/5[a]	15/85/7.5[a]
10/90	10/90/2.5[a]	10/90/5[a]	10/90/7.5[a]
0/100	—	—	—

[a] Indicates the PP-*g*-2-HEMA copolymer as a compatibilizer in the phr level.

(a)

(b)

(c)

Figure 2 Scanning electron micrographs of impact fractured surfaces of the blends: (a) 90/10/2.5* PP/ABS/PP-*g*-2-HEMA; (b) 85/15/2.5* PP/ABS/PP-*g*-2-HEMA; (c) 75/25/2.5* PP/ABS/PP-*g*-2-HEMA.

Flexural properties were measured as per the procedure described in ASTM D790. A three-point loading system with central loading on a single supported beam was used for the measurements. A crosshead speed of 0.28 cm/min was used in all the measurements.

Morphology

The morphology of room-temperature fractured surfaces etched with methyl ethyl ketone (MEK) for ABS extraction was examined using a scanning electron microscope (SEM; Leica Cambridge, UK Stereoscan) at 10 kV. The samples were gold-coated (50 μm thick) using an automatic sputter coater (Polaron Equipment Ltd., USA) to avoid surface charging.

RESULTS AND DISCUSSION

Morphology

The scanning electron micrographs of room-temperature fractured PP/ABS binary blends [Fig. 1(a, b)] do not show any adhesion at the interface. The smoother surface of the cavities observed in the binary blends indicate no adhesion between inclusions and the matrix. This indicates the incompatibility of the phases in spite of the finer and homogeneous dispersion of ABS in the PP matrix. For the blends containing 10% ABS, the particle size was observed to be 10–15 μm, whereas for the blends containing 15% ABS, it was observed to be 20–30 μm. Thus, the size of the dispersed phase was observed to increase with an increasing concentration of the dispersed phase [Fig. 1(a, b)]. However, on addition of the compatibilizer, a marked difference was observed in the morphology of
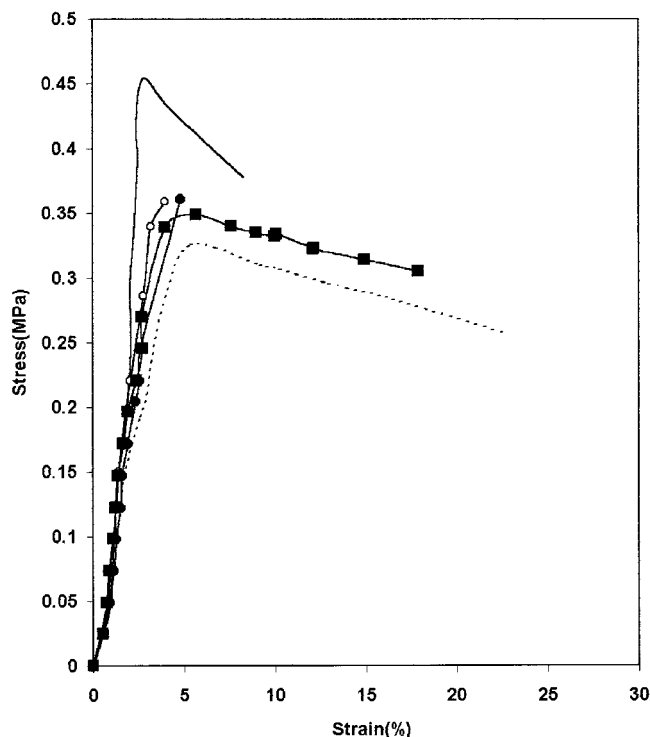

Figure 3 Stress–strain curves of PP/ABS blends: (–) ABS; (----) PP; (■) 90/10/2.5* PP/ABS/PP-*g*-2-HEMA; (●) 85/15/2.5* PP/ABS/PP-*g*-2-HEMA; (○) 75/25/2.5* PP/ABS/PP-*g*-2-HEMA.
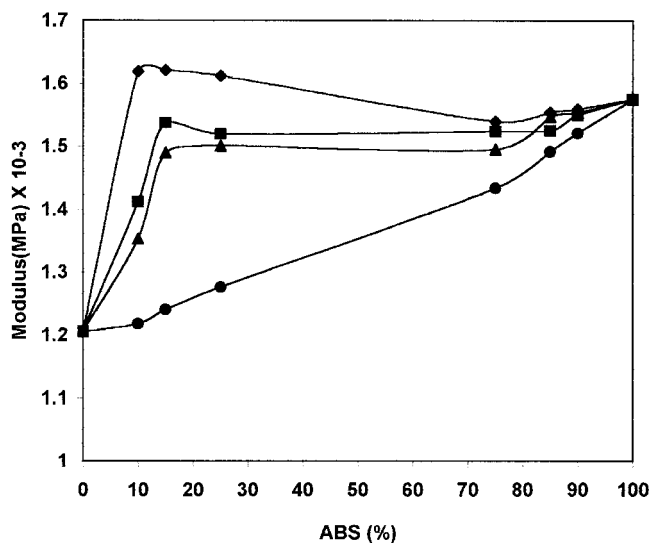
Figure 4 Tensile modulus of PP/ABS blends: (◆) PP/ABS/2.5* PP-g-2-HEMA; (■) PP/ABS/5* PP-g-2-HEMA; (▲) PP/ABS/7.5* PP-g-2-HEMA; (●) PP/ABS (%).

the binary blends. The addition of only 2.5 phr of PP-g-2-HEMA to the PP/ABS binary blends increased the adhesion between the phases and lowered the size of the dispersed phase to 5–10 μm [Fig. 2(a–c)]. The dispersion was observed to be more homogeneous and finer. The surfaces of cavities formed due to the etching of the dispersed phase in MEK were also observed to be rough, indicating greater adhesion at the interface of the phases [Fig. 2(a–c)].

Tensile mechanical properties

Stress–strain curves for the binary PP/ABS and ternary PP/PP-g-2-HEMA/ABS blends are illustrated in Figure 3. It was observed that blends containing 10–15% ABS show ductile behavior, whereas blends with 25% and more ABS break before the yield point, indicating a brittle character.

Due to the lower tensile modulus of PP, the tensile modulus of all binary and ternary blends was observed to be lower than that of ABS (Fig. 4). However, incorporation of PP in ABS does not show a considerable effect on the modulus, but incorporation of ABS in PP shows a considerable increase in the modulus of the ternary blends. The tensile modulus of the ternary blends was observed to be higher than that of the binary blends at all compositions. This may be due to the increased adhesion at the interface and the finer and homogeneous dispersion.

Theoretical background

Many theories have been put forward for the prediction of the elastic modulus of the heterogeneous blends.[29] There are three principal groups of models

that can predict the modulus–composition dependence of blends:

(i) the mechanical coupling model,
(ii) the self-consistent model, and the
(iii) the bounds on modulus model.

Among these, a self-consistent model which is widely used for various blends is based on three assumptions:

- Perfect adhesion exists between the matrix and the inclusions,
- Interinclusion interactions are negligible, and
- The inclusions are spherical.

Based on these assumptions, Kerner[30] proposed the following model for the prediction of tensile modulus (E) of the blends, with the components having similar Poisson's ratios (ν) and perfect adhesion at the boundary:

$$E_b = E_m \frac{\{\phi_d E_d / [(7 - 5\nu_m)E_m + (8 - 10\nu_m)E_m] + \phi_m 15(1 - \nu_m)\}}{\{\phi_d E_m / [(7 - 5\nu_m)E_m + (8 - 10\nu_m)E_d] + \phi_m 15(1 - \nu_m)\}} \quad (1)$$

where E is the tensile modulus; ϕ, the volume fraction; and ν, Poisson's ratio. Subscripts b, m, and d refer to the blend, matrix, and dispersed phase, respectively.

Loosely bound inclusions contribute a little to the overall modulus of blends (E_b). Hence, the observed modulus of such blends is due mainly to the modulus
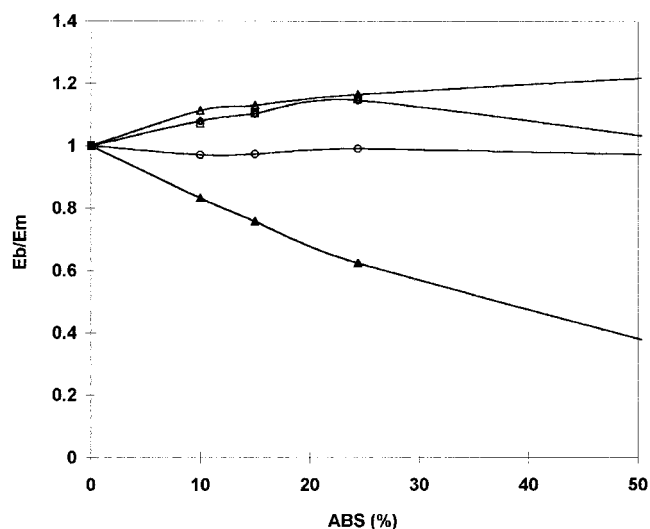

Figure 5 Theoretical models for the tensile modulus: (▲) Kerners model for loosely bound inclusions; (△) Kerners model for perfectly bound inclusions; (□) tesile modulus calculated from Neilsen model for rubber dispersed in the rigid matrix; (○) PP/ABS (%) blends experimental value; (◆) PP/ABS/2.5* PP-g-2-HEMA blends experimental value.

TABLE II
Adjusted ϕ_{max} Values for PP/ABS/PP-g-2-HEMA

ABS (%) in blends	ϕ_{max}			
	2.5 phr PP-g-2-HEMA	5.0 phr PP-g-2-HEMA	7.5 phr PP-g-2-HEMA	0.0 phr PP-g-2-HEMA
10	0.34	0.41	0.48	0.35
15	0.43	0.49	0.52	0.42
25	0.63	0.64	0.67	0.54

of the matrix and the contribution of E_d is negligible ($E_d \cong 0$). As a result, eq. (1) is reduced to

$$\frac{1}{E_b} = \frac{1}{E_m}\left[1 + \frac{\phi_d\,15(1 - \nu_m)}{(7 - 5\nu_m)\,\phi_m}\right] \quad (2)$$

In Kerner's model, only a particle–matrix interaction was considered, but no particle–particle interaction was considered. Therefore, Nielsen[31] modified Kerner's model by considering particle–particle interactions in blends. According to Nielsen's model for the blends containing a rigid polymer dispersed in a rubber matrix, the tensile modulus is given as

$$\frac{E_b}{E_m} = \frac{1 + AB\phi_d}{1 - B\psi\phi_d} \quad (3)$$

where $B = (E_d/E_m - 1)/(E_d/E_m + A)$ and $\psi = 1 + ((1 - \phi_{max})/\phi^2_{max})\phi_d$. For the blends with rubbery particles dispersed in a rigid matrix, the blend modulus is given as

$$\frac{E_m}{E_b} = \frac{1 + AB_i\phi_d}{1 - B_i\psi\phi_d} \quad (4)$$

where $B_i = (E_m/E_d - 1)/(E_m/E_d + A)$ and $\psi = 1 + ((1 - \phi_{max})/\phi^2_{max})\phi_d$. The constant A is $(7 - 5\nu_m)/(8 - 10\nu_m)$ for eq. (3) and $(8 - 10\nu_m)/(7 - 5\nu_m)$ for eq. (4). For PP-rich blends, eq. (4) is applicable.

ϕ_{max} is the maximum packing volume and can be considered as a scale of interaction between two phases. A smaller value of ϕ_{max} represents a larger interface, and a large value of ϕ_{max} represents a smaller interface. To determine the validity of the proposed models for the systems under examination, the tensile modulus of the blends under study was calculated using these models and Poisson's ratios ν for PP and ABS were 0.35 and 0.39, respectively. The calculated tensile modulus values were compared with those obtained experimentally (Fig. 5). It was observed that Kerner's model for loosely bound inclusion shows a considerable deviation from the experimentally obtained data for binary as well as ternary blends. Hence, it can be assumed that some sort of adhesion/interaction exists even in binary blends. This may originate from the stiffening effect, which is attributed to a higher coefficient of thermal expansion of PP as compared to ABS ($1.7 \times 10^{-4}\ k^{-1}$ and $0.8 \times 10^{-4}\ k^{-1}$ for PP and ABS, respectively). As a result,
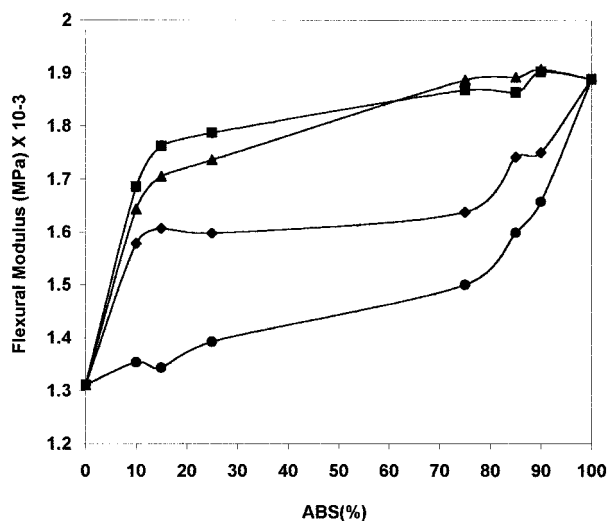

Figure 6 Flexural modulus of PP/ABS blends: (◆) PP/ABS/2.5* PP-g-2-HEMA; (■) PP/ABS/5* PP-g-2-HEMA; (▲) PP/ABS/7.5* PP-g-2-HEMA; (●) PP/ABS (%).
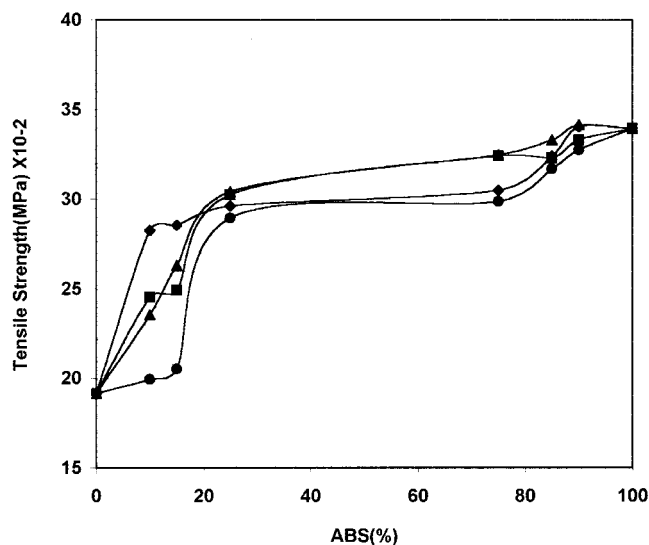

Figure 7 Tensile strength of PP/ABS blends: (◆) PP/ABS/2.5* PP-g-2-HEMA; (■) PP/ABS/5* PP-g-2-HEMA; (▲) PP/ABS/7.5* PP-g-2-HEMA; (●) PP/ABS (%).
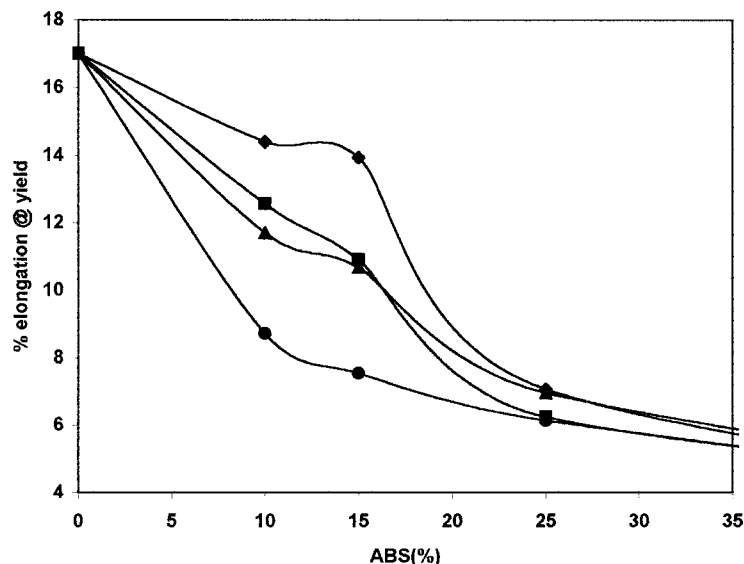
Figure 8 Elongation at yield of PP/ABS blends: (◆) PP/ABS/2.5* PP-*g*-2-HEMA; (■) PP/ABS/5* PP-*g*-2-HEMA; (▲) PP/ABS/7.5* PP-*g*-2-HEMA; (●) PP/ABS (%).

upon solidification, PP contracts more than does ABS. Thus, in PP-rich blends, the ABS phase becomes tightly embedded in the PP matrix, imparting an increased tensile modulus even in binary blends. However, this effect was observed more when a compatibilizer was used. In addition to the stiffening effect, the other factors responsible for the higher tensile modulus in the compatibilized blends are increased homogeneity, finer dispersion, and adhesion at the interface.

Neilsen's model predicts the tensile modulus on the basis of the ϕ_{max} value. The ϕ_{max} values are adjusted in such a way that the theoretical data matches the experimental data. The ϕ_{max} values used for the calculation of the tensile modulus are given in Table II. It was observed that, with an increased content of ABS, ϕ_{max} values continue increasing, indicating an increased volume of the interface, which is immobilized by the discrete phase in the blend. The reciprocal of ϕ_{max} can be considered as an interaction parameter, which is proportional to $(R + \Delta R)^3$, where R is the radius of the inclusion and ΔR is the depth of the interface that is immobilized by the inclusion. For the given value of ΔR, the smaller the size of the inclusion, the smaller the ϕ_{max} value. From Figure 2(a–c), it can be observed that, with an increasing ABS content in the blends, the dispersed particle size increases even in ternary blends, which supports the observed increase in the ϕ_{max} values (Table-II).

The flexural modulus and tensile strength were observed to increase with an increased concentration of ABS in the blends (Figs. 6 and 7). The toughening effect of ABS increases the flexural modulus of the blends. The tensile strength was also observed to increase with an increasing concentration of ABS in the

blends. Due to an increase in the adhesion at the interface, the tensile strength of the ternary blends was observed to be higher compared to the binary blends (Fig. 7).

A sharp decrease in the percent elongation at break was observed in the binary as well as the ternary blends on incorporation of ABS into PP. However, a decrease in the percent elongation was more critical in the binary blends (Fig. 8).

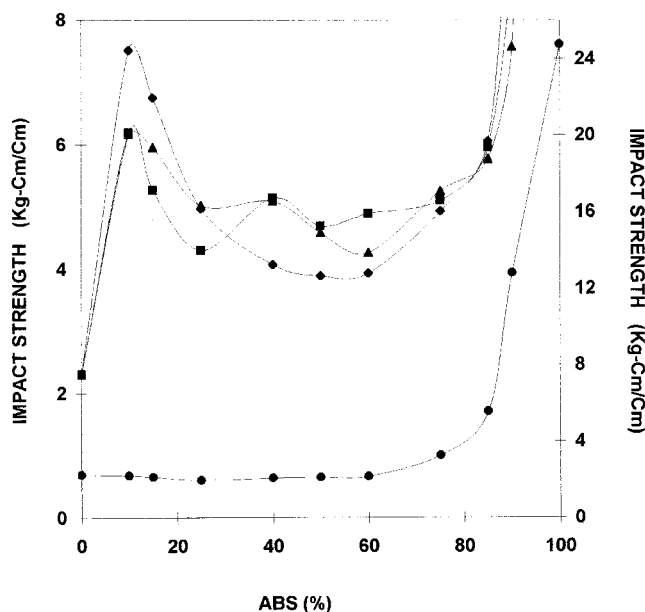Figure 9 illustrates the impact strength of the PP/ABS binary and the PP/PP-*g*-2-HEMA/ABS ternary

Figure 9 Impact strength of PP/ABS blends: (◆) PP/ABS/2.5* PP-*g*-2-HEMA; (■) PP/ABS/5* PP-*g*-2-HEMA; (▲) PP/ABS/7.5* PP-*g*-2-HEMA; (●) PP/ABS (%).

blends as a function of the ABS content in the blends. As seen from Figure 9, the 2.5-phr compatibilizer is sufficient for toughening the blends, which imparts 7.2 kg cm cm^{-1} of notch impact strength at a 90/10 PP/ ABS blend composition, whereas further incorporation of the compatibilizer in the blend does not show improvement in the impact strength but, rather, decreases the impact strength. This can be explained from the observed smaller particle size of the dispersed phase at a 2.5-phr compatibilizer concentration [Fig. 2(a)]. The decrease in the impact strength of the blends with an increase in the compatibilizer concentration can be attributed to the formation of aggregates of the compatibilizer in the bulk phase after a critical concentration of the compatibilizer at the interface. Asaletha et al.[32] and Thomas et al.[33] made a similar observation for PP/NR blends in which the size of the dispersed particle decreases only up to certain concentration of the compatibilizer.

CONCLUSIONS

The use of PP-g-2-HEMA showed an improvement in the Izod impact strength, tensile strength, and tensile modulus properties of PP/ABS bends. The 2.5-phr concentration of the compatibilizer was observed to be critical for the improvement in the properties. Kerner's model for perfect adhesion was observed to be applicable only for PP-rich blends, whereas in Neilsen's model, it was observed that, at a 2.5-phr concentration of the compatibilizer, the values of ϕ_{max} were lower compared to those at a higher compatibilizer content; thus, at a 2.5-phr compatibilizer content, the particle size of the dispersed phase was also lower. Compatibilization of blends resulted into a smaller size of the dispersed phase (ABS) in PP-rich blends.

References

1. Utracki, L. A. Polymer Alloys and Blends, Thermodynamics and Rheology; Hanser: Munich, 1989.
2. Olabishi, O.; Robeson, L. M.; Shaw, S. M. Polymer–Polymer Miscibility; Academic: New York, 1978.
3. Koning, C.; Duin, M. V.; Pagnoulle, C.; Jerome, R. Prog Polym Sci 1998, 23, 707.
4. Paul, D. R. In Polymer Blends I & II; Paul, D. R.; Newman, S., Eds.; Academic: New York, 1978.
5. Utracki, L. A. Commercial Alloys and Blends; Hanser: Munich, 1993.
6. Liang, Z.; William, H. L. J Appl Polym Sci 1991, 43, 379.
7. Sathe, S. N.; Rao, G. S. S.; Rao, K. V.; Devi, S. J Appl Polym Sci 1996, 61, 107.
8. Damoulin, M. M.; Farha, C.; Utracki, L. A. Polym Eng Sci 1984, 24, 1319.
9. Lustiger, A. Can Patent Appl. 2 083 664, 1993.
10. Markin, C.; Williams, H. C. J Appl Polym Sci 1980, 25, 2451.
11. Gupta, A. K.; Jain, A. K.; Maiti, S. N. J Appl Polym Sci 1989, 38, 1699.
12. Gupta, A. K.; Jain, A. K.; Maiti, S. N. J Appl Polym Sci 1990, 39, 515.
13. Frounchi, M.; Burford, R. P. Iran J Polym Sci Technol 1993, 2, 59.
14. Padwa, A. R. Res Discl 1993, 359, 759.
15. Res Discl 1993, 352, 553.
16. Wang, J.; Zhu, C. Sulio 1990, 19, 3.
17. Wang, J.; Zhu, C. C-MRS Int Symp Proc 1990, 3, 131.
18. Osamu, K.; Masahiro, K. Jpn. Patent 06 207 037, 1995 (to Ikeda-Bassan Co.).
19. Hiromasu, K. A. Jpn. Patent 06 248 154, 1995 (to Hitachi Chemical Co. Ltd.).
20. Yamamoto, Y.; Aibe, H. Jpn. Patent 05 93 110, 1993 (to Mitsui Petrochemical Ind.).
21. Padwa, A. R. U.S. Patent 35 082 742, 1992 (to Monsato Co.).
22. TDK Electronics Co. Ltd. Jpn. Patents 82 53 550, 82 53 549, 1982.
23. Patel, A. C.; Brahmbhatt, R. B.; Devi, S. J Appl Polym Sci, in press.
24. Fowler, M. E.; Barlow, J. W.; Paul, D. R. Polymer 1987, 28, 1177.
25. Lee, P. C.; Kuo, W. F.; Chang, F. C. Polymer 1994, 35, 564.
26. Sasaki, I.; Yanagase, A.; Kawachi, Y.; Mayuzumi, T.; Oba, T.; Okada, F. U.S. Patent 4 69 086, 1987.
27. Dean, B. D. J Elastom Plast 1985, 17, 55.
28. Patel, A. C.; Brahmbhatt, R. B.; Devi, S. J Appl Polym Sci 1998, 69, 2107.
29. Dickie, R. A. In Polymer Blends; Paul, D. R.; Newman, S.; Eds.; Academic: New York, 1978.
30. Kerner, E. A. Proc Phys Soc B 1950, 69, 808.
31. Nielsen, E. Mechanical Properties of Polymer and Composites; Marcel Dekker: New York, 1974.
32. Asaletha, R.; Kumaran, G.; Thomas, S. Rubb Chem Technol 1995, 68, 671.
33. Thomas, S.; Praud 'Homme, R. E. Polymer 1992, 33, 4260.